I&EC research
Industrial & Engineering Chemistry Research

Article

Cite This: Ind. Eng. Chem. Res. 2018, 57, 10663−10674

pubs.acs.org/IECR

Combined Steam Reforming of Methane and Formic Acid To Produce Syngas with an Adjustable H_2:CO Ratio

Ahmadreza Rahbari, Mahinder Ramdin, Leo J. P. van den Broeke, and Thijs J. H. Vlugt*

Engineering Thermodynamics, Process & Energy Department, Faculty of Mechanical, Maritime and Materials Engineering, Delft University of Technology, Leeghwaterstraat 39, 2628CB Delft, The Netherlands

Supporting Information

ABSTRACT: Syngas is an important intermediate in the chemical process industry. It is used for the production of hydrocarbons, acetic acid, oxo-alcohols, and other chemicals. Depending on the target product and stoichiometry of the reaction, an optimum (molar) ratio between hydrogen and carbon monoxide (H_2:CO) in the syngas is required. Different technologies are available to control the H_2:CO molar ratio in the syngas. The combination of steam reforming of methane (SRM) and the water-gas shift (WGS) reaction is the most established approach for syngas production. In this work, to adjust the H_2:CO ratio, we have considered formic acid (FA) as a source for both hydrogen and carbon monoxide. Using thermochemical equilibrium calculations, we show that the syngas composition can be controlled by cofeeding formic acid into the SRM process. The H_2:CO molar ratio can be adjusted to a value between one and three by adjusting the concentration of FA in the reaction feed. At steam reforming conditions, typically above 900 K, FA can decompose to water and carbon monoxide and/or to hydrogen and carbon dioxide. Our results show that cofeeding FA into the SRM process can adjust the H_2:CO molar ratio in a single step. This can potentially be an alternative to the WGS process.

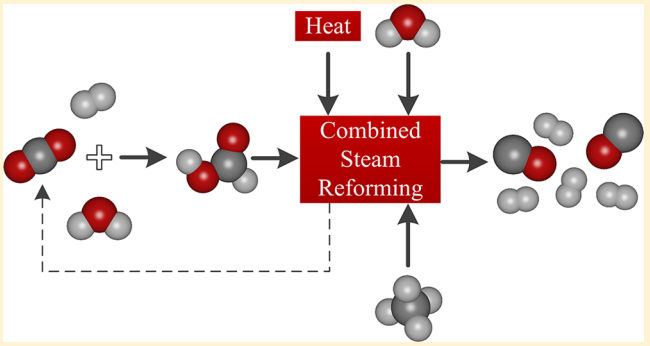

1. INTRODUCTION

One of the consequences of the energy transition is that fossil fuel based production of chemicals will be replaced with renewable energy based processes.[1−3] The current infrastructure for producing chemicals is predominantly based on hydrogen and carbon. This means that to support the energy transition, a widely available and sustainable C_1 source is required. Therefore, the reuse of carbon dioxide will be an essential part of future chemical production processes.[4−7] A range of efforts are underway to use carbon dioxide as a sustainable and economical source of C_1 to produce value-added chemicals.[5−8] There are basically two pathways for the conversion of carbon dioxide: either by conventional hydrogenation or by electrochemical conversion.

Formic acid (FA) is one of the simplest products that can be made from carbon dioxide.[8] Recently, FA production by electrochemical reduction of CO_2 has gained significant interest.[7,9−13] In this process, the overall reaction in the electrochemical cell is the conversion of carbon dioxide with water to FA according to

$$CO_2 + H_2O \rightarrow HCOOH + \frac{1}{2}O_2 \quad \text{(R1)}$$

The main advantage of the electrochemical conversion of carbon dioxide is that in the reaction water can be used as the hydrogen source. The cathodic half-cell reduction of carbon dioxide is described by the following reaction:[11]

$$CO_2 + 2H^+ + 2e^- \rightarrow HCOOH \quad \text{(R2)}$$

The formation of FA is a two electron reaction, and the electric power to convert 1 kg of carbon dioxide to FA follows from[14]

$$P = \frac{IU}{M_{CO_2}} \quad (1)$$

$$= \epsilon\frac{\lambda FQU}{tM_{CO_2}} \quad (2)$$

where P is the power input in kWh per kg carbon dioxide, I (A) is the electric current, U is the electrical potential which is on the order of 2.2−2.5 (V), λ is the number of electrons, λ = 2, F is the Faraday coefficient which is equal to 96485 C $mol^{-1}_{electron}$, Q (C) is the total electric charge provided to the reactor, t (s) is the time, and M_{CO_2} (g mol^{-1}) is the molecular mass of carbon dioxide. For an overall energy efficiency, ϵ, of around 70%, the energy required to convert 1 kg of carbon

Received: May 31, 2018
Revised: July 16, 2018
Accepted: July 17, 2018
Published: July 17, 2018

DOI: 10.1021/acs.iecr.8b02443
Ind. Eng. Chem. Res. 2018, 57, 10663−10674

dioxide into 1 kg of FA is ca. 4 kWh.[15] A simple gross profit analysis using $5 per kg carbon dioxide and an electricity price of $5 per kWh leads to a cost price of around $25 per kg FA.[16]

For the hydrogenation reactions, the most sustainable approach to produce the required hydrogen is by water electrolysis, while traditional hydrogen production methods are based on fossil fuels.[5,17] The conventional catalytic hydrogenation of carbon dioxide to FA proceeds according to[4,18]

$$CO_2 + H_2 \rightarrow HCOOH \quad (R3)$$

FA is the simplest C_1 carboxylic acid, it is a nontoxic liquid between 281.55 and 373.15 K, and it can be safely stored in aqueous solutions.[19,20] In addition, hydrogenation of biomass derived feedstocks has been suggested as potential sustainable pathways to formate/formic acid production.[6,21−26] Alternatively, value-added chemicals such as methanol, dimethyl ether, and formate/formic acid can be produced by hydrogenation of carbon dioxide.[4,18] To date, FA is mainly considered as a hydrogen storage material via its decomposition to hydrogen and carbon dioxide.[4,27−44] One of the key observations is that FA can be considered as a carbon monoxide carrier as well via its decomposition to water and carbon monoxide.[41,42] Basically, by combining the two main decomposition pathways toward hydrogen and carbon monoxide, and additional products such as water and carbon dioxide, FA can therefore be considered as a source for syngas. Yoshida et al. have reported the presence of FA as an intermediate in the water-gas shift reaction (WGS) reaction reaction:[20,45,46]

$$H_2 + CO_2 \rightleftharpoons HCOOH \rightleftharpoons H_2O + CO \quad (R4)$$

On a molecular weight basis, FA contains 4.3 wt % hydrogen and 60.9 wt % carbon monoxide. Using a FA density of 1.22 kg L^{-1} at standard conditions leads to 53 g H_2 per liter FA and 744 g of carbon monoxide per liter FA. Based on the amount of 4.3 wt % or 53 g of hydrogen, FA is identified as one of the most promising candidates for hydrogen storage.[38,47−49] Considering the high carbon monoxide fraction in FA, it is interesting to explore the potential of FA as carbon monoxide carrier.

Typically, the WGS reaction is used together with steam reforming of methane (SRM) to adjust the composition of the synthesis gas (syngas). This is one of the most common and oldest methods for syngas production.[5,50−56,58,59] The reaction pathways for the SRM and WGS are

$$CH_4 + H_2O \rightleftharpoons CO + 3H_2 \quad (R5)$$

$$CO + H_2O \rightleftharpoons CO_2 + H_2 \quad (R6)$$

Comparing reactions R4 and R6 shows that by cofeeding FA to the SRM process, the WGS and the SRM reactions can be performed in a single step.

In this work, we show that by using thermochemical equilibrium calculations, the syngas composition (the H_2:CO molar ratio) can be adjusted to any required value between one and three by cofeeding FA to the SRM reaction. FA in the reactant feed decomposes to water and carbon monoxide and/or to hydrogen and carbon dioxide which are all involved in the WGS reaction at high temperatures. This can potentially change the conventional SRM and WGS reactions (R5 and R6) from a two-step process into a single-step process.

This paper is organized as follows. In section 3, thermodynamic modeling of reactions R4 and R5 is explained in detail. The Gibbs free energies of each component is calculated at standard pressure and temperatures between 400 and 1400 K based on the partition function of isolated molecules. The Gibbs minimization method is used to calculate the composition of the product syngas at chemical equilibrium. Our results are summarized in section 4. It is shown that the H_2:CO molar ratio can be adjusted to any value between one to three based on the initial concentration of the FA in the feed. Our conclusions are summarized in section 5.

2. APPLICATIONS OF FORMIC ACID

2.1. Formic Acid Decomposition. The decomposition of FA can proceed according to two different pathways: decarbonylation (or dehydration) into carbon monoxide and water or decarboxylation (dehydrogenation) into hydrogen and carbon dioxide:

$$HCOOH \rightleftharpoons H_2O + CO \quad (R7)$$

$$HCOOH \rightleftharpoons H_2 + CO_2 \quad (R8)$$

The selectivity toward FA dehydration or dehydrogenation depends on the temperature, pressure, and the type of catalyst. For the heterogeneous FA decomposition, the dehydration/dehydrogenation selectivity of different solid catalysts has been studied.[39,60] Metals and zinc oxide are predominantly active for reaction R8, while other oxides are predominantly active for reaction R7.[60] Lopez et al. reported the results for different catalysts used for the heterogeneous FA decomposition reactions in the temperature range of T = 573−673 K.[39]

Blake and Hinshelwood investigated the homogeneous decomposition of FA acid in the gas phase for temperatures between T = 709 and 805 K and concluded that catalytic effects become negligible at temperatures above T = 773 K.[41] Therefore, reactions R7 and R8 are assumed to be in equilibrium at high temperatures, which is a reasonable assumption since kinetics are fast and of minor importance.[41] In the temperature range of T = 709 and 805 K, it was observed that reaction R8 is of first-order while reaction R7 is of second-order. The reaction rates for packed and unpacked reactors were essentially the same for reactions R7 and R8. In the beginning of the 1970s, Blake et al. extended the experiment to the temperature range of T = 820−1053 K.[42] In this temperature range, reaction R8 was also observed to be a minor process, with typical CO:CO_2 = 10:1 molar ratios. Reaction R7 is of second-order for temperatures below T = 943 K and has an order of 1.5 for higher temperatures. The difference in yield of CO and CO_2 was attributed to the water-gas shift reaction.

2.2. Synthesis of Formic Acid. Current industrial synthesis of FA is mainly based on fossil feedstocks using methanol carbonylation/methyl formate hydrolysis and naphtha partial oxidation.[47] On a large scale, FA is produced in a two-step process of methanol carbonylation followed by methyl formate hydrolysis. In 2014, this two-step process was used to produce 81% of FA acid worldwide.[61] In the first step, carbon monoxide reacts with methanol at pressures around P = 4 MPa and temperatures around T = 353 K to produce methyl formate. FA and methanol are produced in the second step by methyl formate hydrolysis. The produced methanol is recycled back to the first step:[25,61]

$$CO + CH_3OH \rightarrow HCOOCH_3 \quad (R9)$$

$$HCOOCH_3 + H_2O \rightarrow HCOOH + CH_3OH \quad (R10)$$

DOI: 10.1021/acs.iecr.8b02443
Ind. Eng. Chem. Res. 2018, 57, 10663−10674

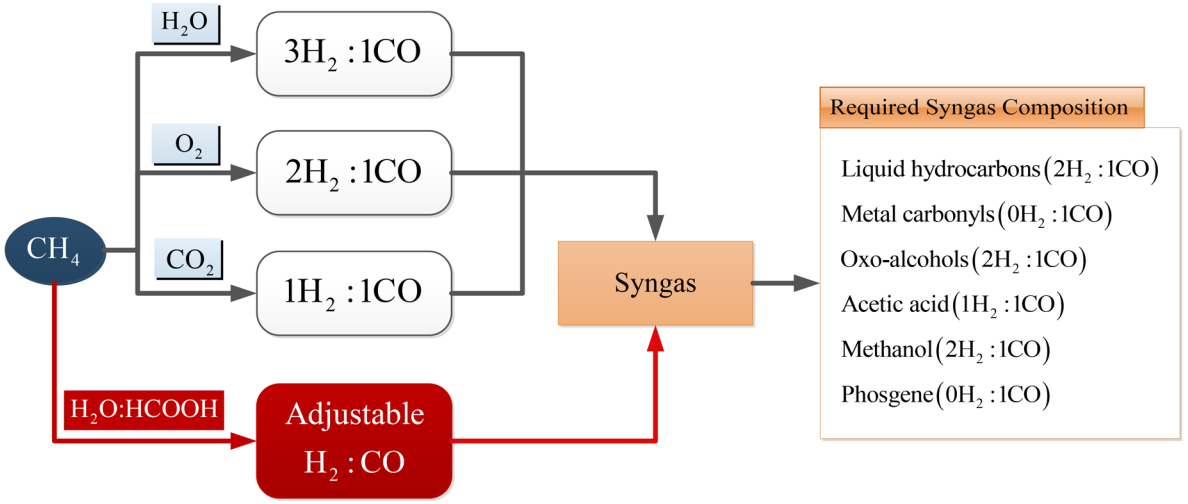

Figure 1. Different reaction pathways to reduce methane to syngas using oxygen (R12), steam (R5), carbon dioxide (R11), and an aqueous mixture of FA (R4) (proposed in this work). Syntheses of different products require favorable syngas H_2:CO ratios.[145] Synthesis of liquid hydrocarbons using the FT reaction (H_2:CO = 2:1),[51] metal carbonyls, oxo-alcohols (H_2:CO = 1:1),[81] acetic acid (H_2:CO = 1:1),[82] methanol synthesis (H_2:CO = 2:1),[73] and phosgene (H_2:CO = 0:1).[146]

The sum of reactions R9 and R10 reduces to the direct reaction of carbon monoxide with water. FA synthesis based on methanol is a reliable and established process; however, it has some drawbacks.[25,61] The process uses carbon monoxide produced at high temperatures which is very energy intensive.[25] Also, a large excess of water is required to decompose methyl formate to FA (R10).[25] The main application of FA is for the production of preservatives and as antibacterial agent;[62] it is also used for dyeing in the leather industry. FA has received increased attention as a suitable material for controlled hydrogen storage and release.[19,47,62−65] A relatively new application is the use of FA in direct formic acid fuel cells (DFACF).[66,68,69] It has also been proposed to use FA for storage and transportation of carbon monoxide[70] or carbon dioxide.[62,71]

2.3. Established Syngas Technologies. Syngas refers to gas phase mixtures of hydrogen and carbon monoxide with various H_2:CO ratios.[5,52,53] Syngas can be produced by reforming almost any hydrocarbon source, such as naphtha, heavy oil, natural gas, biomass, or coal.[52,56] Currently, steam reforming of light hydrocarbons (e.g., methane, ethane, methanol, and ethanol) is the most commonly used method for syngas production.[5,50−56,58,59] An alternative source for syngas production are coal reserves; however, the investment costs associated with a coal-based syngas plant are approximately 3 times higher as compared to a natural gas-based plant.[56] Therefore, natural gas remains the major source for syngas production.[5,56] Syngas is an intermediate in many industrial applications, and depending on the downstream process, the optimal H_2:CO molar ratio required in the syngas typically lies between one and three.[51,72] The most common syngas applications in the chemical process industry are methanol synthesis (H_2:CO = 2:1),[51,73] Fischer−Tropsch (FT) synthesis (H_2:CO = 2:1),[74−76] oxo-synthesis or hydroformylation (H_2:CO = 1:1),[77−81] and acetic acid synthesis (H_2:CO = 1:1).[82] As an illustrative example, Figure 1 shows different reaction pathways leading to various syngas compositions by partial oxidation, steam reforming, carbon dioxide reforming, and the combined FA and steam option, as outlined in this work.

To produce syngas from methane, various technologies have been developed, such as SRM[5,58] and WGS,[5,58] carbon dioxide reforming of methane (CRM),[5,58] catalytic partial oxidation of methane (POM),[74,75,81,83] combined partial oxidation and carbon dioxide reforming of methane or autothermal reforming of methane (ARM),[84,85] combined steam reforming, and carbon dioxide reforming of methane (CSRCRM).[53,86]

The first industrial SRM plant was commissioned in the early 1930s.[87,88] Methane is a very stable molecule, and only at relatively high temperatures a high conversion rate to syngas is obtained.[56,89] Syngas production from methane is divided into two steps. First, at high temperatures ranging from T = 1073 to 1273 K and pressures ranging from P = 20 to 40 bar, the SRM reaction takes place. Second, the WGS is performed after the SRM reaction to adjust the H_2:CO molar ratio.[51,58,90] SRM is typically performed using Ni-based catalysts.[5] This is related to the low cost and favorable activity of the Ni-based catalysts as compared to noble metals.[59,91] Although noble metals are more coke resistant,[56] the high cost and the limited availability make Ni catalysts a more practical choice in commercial applications.[92] SRM has two major drawbacks. In particular, the Ni-based processes suffer from coke formation which leads to deactivation of the catalyst. To avoid coke formation on the catalyst surface, excess steam is added which results in H_2 enriched syngas,[93] and this will lead to a syngas composition with a H_2:CO molar ratio larger than three.[54,55,84,94] The syngas compositions with high H_2:CO molar ratios do not meet the requirements for many downstream petrochemical processes, e.g., FT synthesis,[56,74,75,88] acetic acid synthesis,[88] or methanol synthesis.[72,94−97] The other disadvantage is that the SRM reaction is highly endothermic and subsequently highly energy intensive.[51,89,94,98,99]

Alternatively, in CRM (dry reforming), steam is replaced by carbon dioxide:[58]

$$CH_4 + CO_2 \rightarrow 2H_2 + 2CO \qquad \text{(R11)}$$

CRM is a CO_2-consuming reaction at temperatures between T = 1073 and 1273 K, resulting in syngas with H_2:CO = 1:1 molar ratio.[5,56,100−102] This syngas composition is more suitable for some downstream processes.[56,74,75,100,101] To

DOI: 10.1021/acs.iecr.8b02443
Ind. Eng. Chem. Res. 2018, 57, 10663−10674

lower the H_2:CO molar ratio of the syngas, CRM is widely used as a secondary reforming reaction after the SRM reaction.[103] CRM synthesis using Ni-based catalysts, Co-based catalysts, and noble-metal-based catalysts are reported extensively in the literature.[83,100,102] The main drawback of the CRM reaction is the rapid coke deposition, which can be explained by the Boudouard reaction[56,104] ($2CO \rightarrow C + CO_2$) taking place on the catalyst surface. Another disadvantage is the direct decomposition of methane[56,104] ($CH_4 \rightarrow C + 2\ H_2$) at high concentrations of CO_2 in the feed.[5,83,100,103,105]

Catalytic partial oxidation of methane (POM), also known as oxy-reforming, was introduced as an alternative to obtain syngas with a H_2:CO = 2:1 molar ratio, suitable for producing long chain hydrocarbons,[5,74,75] and as a feed for methanol synthesis.[94−96]

$$CH_4 + \frac{1}{2}O_2 \rightarrow CO + 2H_2 \quad \text{(R12)}$$

POM is favorable for a wide range of temperatures allowing close to 100% methane conversion to syngas.[89,106] The advantages include a short residence time and mild exothermicity.[53,56,76,88,94,107] The main drawback is the presence of hot spots as a result of the high conversion rates of methane.[53,76,92,93,108,109] Removing the heat produced in the reactor is difficult for large-scale operations, making the process difficult to control. From experiments by Prettre et al. it was shown that the catalytic oxidation of methane, with reactant feed composition CH_4:O_2 = 2:1, is not accurately represented by (R12).[106,110] It seems that the POM reaction proceeds in two steps. The first step is exothermic which involves deep oxidation (combustion) of a part of the methane (approximately 25% of the starting moles) to carbon dioxide and steam. All oxygen is consumed during this process. In the second step, the residual methane reduces steam and carbon dioxide to syngas.[89,94,106,107,110] This is an endothermic process. The POM reaction mechanism can be described by the following three reactions:[106,110]

$$CH_4 + 2O_2 \rightarrow CO_2 + 2H_2O \quad \text{(R13)}$$

$$CH_4 + H_2O \rightleftharpoons CO + 3H_2 \quad \text{(R14)}$$

$$CH_4 + CO_2 \rightleftharpoons 2CO + 2H_2 \quad \text{(R15)}$$

The overall sequence of reactions (R13−R15) using a Ni/Al_2O_3 catalyst results in syngas with a H_2:CO = 2:1 ratio as reported by Dissanayake et al.[106] Yamamoto et al. have proposed the same reaction mechanism for partial oxidation of C_6^+ hydrocarbons using supported Ni catalysts.[106,111] Different combinations of feedstock and catalysts can provide a specific H_2:CO molar ratio.[58,109]

Autothermal reforming of methane (ARM) is a combination of the POM and SRM-CRM process.[112−115] ARM is performed either in one or two separate reactors to reduce the energy consumption.[5,58] The combination of the exothermic POM and endothermic SRM is energetically favorable.[85] ARM was originally designed for syngas production in ammonia and methanol plants in the 1950s.[57] The oxygen-steam flow is mixed with methane typically at around T = 2200 K,[56] and methane is oxidized in a substoichiometric flame. Combustion products enter the catalyst bed reactor with high thermal stability and with the temperature in the range of T = 1200−1400 K:[56,57]

$$CH_4 + H_2O \rightleftharpoons CO + 3H_2 \quad \text{(R16)}$$

$$CH_4 + \frac{3}{2}O_2 \rightarrow CO + 2H_2O \quad \text{(R17)}$$

Adding steam is crucial for the ARM process as it prevents explosion hazards and suppresses coke formation.[5,85] Equilibration of the syngas is further governed by the SRM and WGS reactions.[57] The H_2:CO molar ratio in the syngas can be precisely controlled by adjusting the H_2O:CH_4 and O_2:CH_4 molar ratios in the feed.[56]

Combined steam and carbon reforming of methane (CSCRM) was proposed as an alternative to directly control the syngas composition.[53,86] In this process, the H_2:CO molar ratio is adjusted by partially cofeeding carbon dioxide and steam with the reaction feed. Adding steam to CRM process drastically reduces coke deposition on the catalyst.[83,116] By changing the H_2O:CO_2:CH_4 ratio in the reaction feed, a H_2:CO ratio in the syngas between 1.5 and 2.5 is obtained.[53,57,76,83,93,94,116−118]

3. MODELING AND METHODOLOGY

For a single chemical reaction, the composition of the reaction product at chemical equilibrium is calculated from the method of equilibrium constants.[119−122] In this approach, mole fractions are expressed as functions of a single variable called the reaction coordinate (ϵ). The equilibrium constant is related to the individual mole fractions of the components and the stoichiometric coefficients. Therefore, ϵ is calculated for a single reaction.[119,122] The method of equilibrium constants becomes numerically more difficult as the number of chemical species and reactions increases.[120,122,123]

A necessary condition for chemical equilibrium is that the total Gibbs energy of the mixture reaches a minimum value at a given temperature and pressure. Based on this principle, the Gibbs minimization method[119,122,124] is used as a robust method to compute the composition of the reaction product at chemical equilibrium for multicomponent systems with simultaneous reactions.[119,122,124,125] The solution obtained based on this method is less sensitive to the initial guess as compared to other methods.[119,122,124] The composition of the reaction product at chemical equilibrium is obtained by changing the initial composition such that the Gibbs energy of the mixture is minimized. The total number of atoms of each type should remain constant during this minimization process. The Gibbs free energy, or the chemical potential, of each component at the standard reference pressure, P° = 1 bar, can be evaluated from the isolated molecule partition function:[126−129]

$$\mu^\circ(T) = -RT \ln\left[\left(\frac{q(V, T)}{V^\circ}\right)\frac{k_B T}{P^\circ}\right] \quad (3)$$

with $q(V,T)/V^\circ$ the temperature-dependent part of the ideal gas partition function, k_B is the Boltzmann constant, P° is the standard reference pressure (1 bar), T is the temperature, and the volume $V^\circ = k_B T/P^\circ$. Details regarding the calculation of the reference chemical potential from eq 3 are provided in the Supporting Information.[129] The total Gibbs energy of a multicomponent mixture equals[122,130,131]

$$G^t = \sum_{i=1}^{S} n_i \mu_i \quad (4)$$

where G^t is the total Gibbs energy of the mixture, S is the number of components in the mixture, n_i is the number of

DOI: 10.1021/acs.iecr.8b02443
Ind. Eng. Chem. Res. 2018, 57, 10663−10674

moles of component i, μ_i is the chemical potential of component i in the mixture, and S is the total number of components in the mixture. Considering the standard state as an ideal gas, the chemical potential at any temperature and pressure is obtained from[129,132]

$$\mu_i = \mu_i^\circ + RT \ln \frac{y_i \varphi_i P}{P^\circ} \tag{5}$$

where R is the universal gas constant, y_i is the mole fraction of component i, and φ_i is the fugacity coefficient of component i. The fugacity coefficient can be obtained from experimental volumetric data or an equation of state.[133] Combining eqs 4 and 5 yields

$$G^t = \sum_{i=1}^{S} n_i \mu_i^\circ + RT \sum_{i=1}^{S} n_i \ln \frac{y_i \varphi_i P}{P^\circ} \tag{6}$$

At chemical equilibrium, the function G^t reaches a minimum. In a closed system, the minimization of eq 6 is subject to the constraints of the material balance.[119,122,124] In other words, the number of moles of each atom type remains constant during the reaction. For k types of atoms in the mixture, k independent mass balance equations are applied as constraints:

$$\sum_{i=1}^{S} n_i \alpha_{ik} = A_k \tag{7}$$

where A_k is the number of atoms of type k and α_{ik} is the number of atoms of type k present in molecule type i. Therefore, calculating the mixture composition at chemical equilibrium is reduced to minimizing eq 6 subject to the constraint of eq 7. The objective function, eq 6, is minimized using the function *fmincon* implemented in the MATLAB Optimization Toolbox.[134] In every iteration, the Peng–Robinson equation of state (PR-EoS)[133,135,136] is used to evaluate the fugacity coefficients φ_i in eq 6. The mixture parameters are based on pure component parameters and van der Waals mixing rules.[137,138] The effects of the binary interaction parameters (BIPs) are negligible for gaseous mixtures at high temperatures.[132] Therefore, the BIPs are set to zero in this work. Further details of the PR-EoS modeling and pure component parameters are provided in the Supporting Information. The standard Gibbs energies of reactions R5–R8 at P° are obtained based on the computed chemical potentials of individual components, eq 3, and the corresponding stoichiometric coefficients of the reaction

$$\Delta G_r^\circ = \sum_{i=1}^{S} \nu_i \mu_i^\circ(T) \tag{8}$$

where ν_i is the stoichiometric coefficient of component i. The standard reaction enthalpy ΔH_r° is directly computed using the Gibbs–Helmholtz equation:[126]

$$\left(\frac{\partial \Delta G_r^\circ / T}{\partial T}\right)_P = -\frac{\Delta H_r^\circ}{T^2} \tag{9}$$

4. RESULTS AND DISCUSSION

4.1. Main Reactions. In Figure 2, the values for ΔG_r° and ΔH_r° (eqs 8 and 9) are plotted as a function of the temperature. The data in Figure 2 are obtained for reactions R5–R8. For more details on the computing of ΔG_r° and ΔH_r°, the reader is referred to the Supporting Information. The SRM

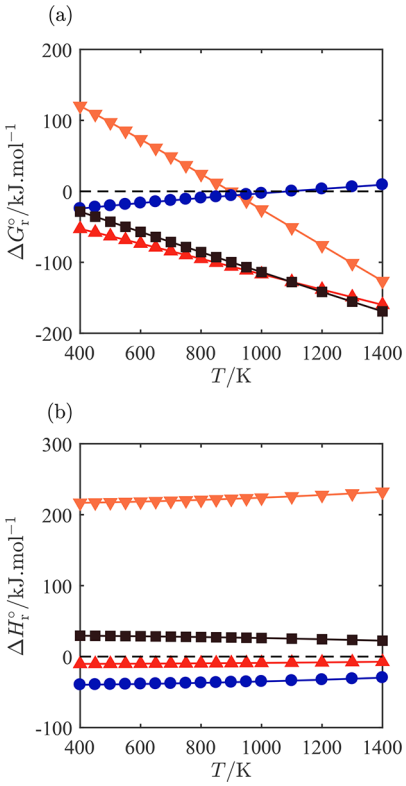

Figure 2. (a) Standard Gibbs energies of reaction and (b) reaction enthalpies for reactions R7 and R8 (per mole of FA), reaction R5 (per mole of methane), and reaction R6 (per mole of water) as a function of temperature at P° = 1 bar. The equilibrium constant is related to the Gibbs free energy change of the reaction.[122,126] The symbols indicate SRM (downward-pointing triangles), WGS (circles), dehydration of FA (squares), and dehydrogenation of FA (upward-pointing triangles). A dashed line is used as a reference line at zero. Standard Gibbs energies of carbon monoxide, water, carbon dioxide, hydrogen, and FA are provided in Table S1 of the Supporting Information.

reaction (R5) is endergonic, $\Delta G_r^\circ > 0$, at temperatures below T = 880 K,[89] and exergonic, $\Delta G_r^\circ < 0$, at temperatures above T = 880 K. This indicates that the syngas production in the SRM reaction is favorable at high temperatures. The FA decomposition reactions (R7 and R8) are also endergonic for the temperature range of T = 400–1400 K. Therefore, thermodynamic equilibrium favors high conversion of FA to water, hydrogen, carbon dioxide, and carbon monoxide at high temperatures.[41,42] The WGS reaction is endergonic at temperatures above T = 1100 K. At high enough temperatures, higher conversion of carbon dioxide and hydrogen to carbon monoxide and water is favored.[139,140] The reaction enthalpies are calculated directly from the Gibbs–Helmholtz equation (eq 9). From the reaction enthalpies, ΔH, it is clear that reactions R5 and R7 are endothermic and reactions R6 and R8 are exothermic.

The Gibbs minimization method is used to compute the syngas equilibrium composition for the SRM and WGS reactions (R5 and R6). The reaction is studied with an equimolar feed mixture of water and methane, H_2O:CH_4 = 1:1, in the temperature range of T = 800–1500 K at P = 1 and 25 bar. The results are shown in Figure 3. As expected, the H_2:CO molar ratios in the syngas are larger than three for the two pressures. It follows from Figure 3 that full conversion of

DOI: 10.1021/acs.iecr.8b02443
Ind. Eng. Chem. Res. 2018, 57, 10663–10674

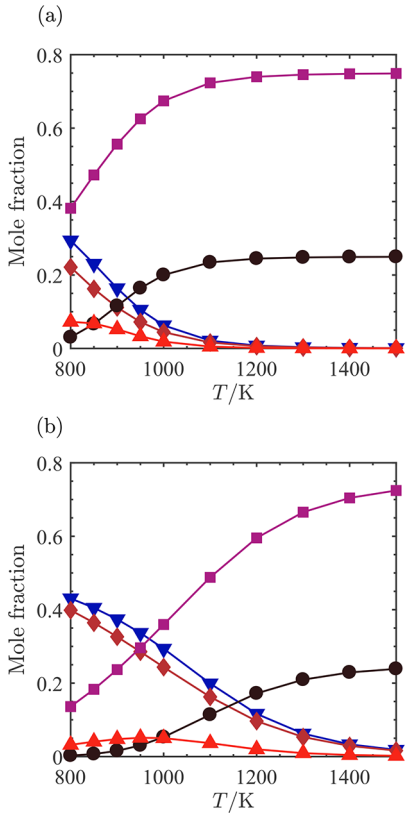

Figure 3. Equilibrium composition of syngas as a function of temperature computed using the Gibbs minimization method (reactions R5 and R6): (a) at pressure of 1 bar and H_2O:CH_4 = 1:1 and (b) at pressure of 25 bar and H_2O:CH_4 = 1:1. In both panels: mole fractions of hydrogen (squares), mole fractions of carbon monoxide (circles), mole fractions of methane (downward-pointing triangles), mole fractions of water (diamonds), and mole fractions of carbon dioxide (upward-pointing triangles).

methane is achieved at T = 1200 K at P = 1 bar, while nearly full conversion of methane at P = 25 bar is not achieved until temperatures above T = 1500 K. For both pressures, low concentrations of carbon dioxide are observed in the syngas mixture at high temperatures. This is because the WGS equilibrium shifts toward carbon monoxide and water at high temperatures.[51,139−141]

4.2. FA Combined with the SRM Process: SRM-FA. To reduce the carbon footprint of hydrogen and syngas production, alternative process schemes need to be developed. In Figure 4, we propose a process scheme in which FA is combined with the SMR process to provide a wide range of H_2 to CO ratios. In this way both the CH_4:H_2O and the HCOOH:H_2O molar ratios can be varied. By using essentially both CH_4 and CO_2 as the C_1 feedstock, the overall consumption of methane will be reduced.

For existing hydrogen and syngas production processes, there are two sources of carbon dioxide. To obtain the required product specifications for the hydrogen or the syngas, pressurized carbon dioxide is removed from the SRM and the WGS processes. Additionally, carbon dioxide is produced during heat generation and is present in the flue gas stream. The pressurized carbon dioxide stream from the existing hydrogen or syngas production units can be used as feedstock for the synthesis of FA, for both the electrochemical conversion and the hydrogenation of carbon dioxide. It should be noted that large scale conversion of carbon dioxide to FA is not yet available. The advantage of the electrochemical route is that the product will be an aqueous FA stream. Various aqueous FA solutions, with different FA wt %, can be fed to the SRM-FA process, where the final syngas composition can be adjusted by the operating conditions for the pressure and temperature.

From the SRM process, syngas with a molar ratio of H_2:CO = 3:1 is generally obtained. However, for most applications a lower H_2:CO molar ratio is required (see Figure 1). To assess

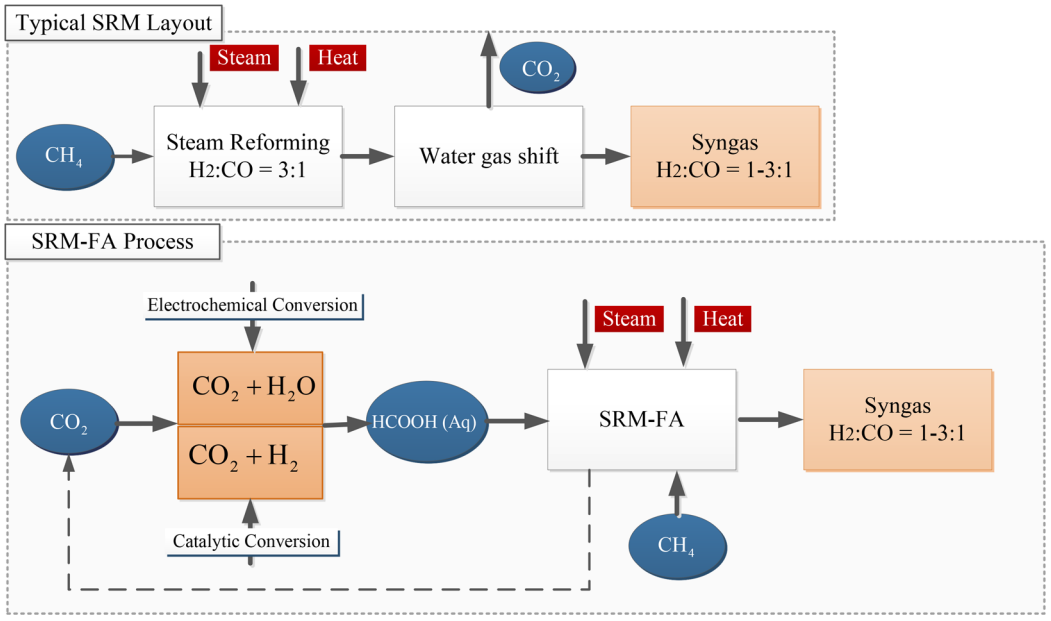

Figure 4. Comparison between a typical SRM layout and the layout for the proposed combined SRM-FA process. In the exiting SRM process, steam reforming is followed by the WGS process to adjust the H_2:CO ratio. In the alternative process, first FA is synthesized, and second the FA is added to the SMR to adjust the H_2:CO ratio. FA can be synthesized either by electrochemical conversion of CO_2[9−13] or by conventional catalytic hydrogenation of CO_2.[4,18]

DOI: 10.1021/acs.iecr.8b02443
Ind. Eng. Chem. Res. 2018, 57, 10663−10674

the potential of FA as a carbon monoxide carrier, the thermodynamic equilibrium of combining the FA decomposition reactions and the SRM reaction was evaluated. The composition of the feed mixture was defined by the molar ratio between water and methane, H_2O:CH_4, and varying the molar ratio between FA and water, HCOOH:H_2O. Two cases for the H_2O:CH_4 molar ratio are considered: H_2O:CH_4 = 1:1 and H_2O:CH_4 = 2:1. For the FA, a HCOOH:H_2O molar ratio in the range from 0.49 to 5.66 has been used (see Table 1). The equilibrium composition of the syngas is calculated using the Gibbs minimization method based on reactions R4 and R5.

Table 1. Different Molar Ratios of FA in FA−Water Mixtures Used in the Reactant Feed[a]

FA:H_2O	FA:(FA + H_2O) (%)	FA (wt %)
0.11	10	22
0.49	33	56
1.00	50	72
1.50	60	79
5.66	85	94

[a]The corresponding mole percentage and weight percentage of FA (wt %) in the mixture is calculated based on the molar ratio between FA and water. The molar ratios between water and methane used in the simulations are H_2O:CH_4 = 1:1 and H_2O:CH_4 = 2:1.

The results for the equilibrium syngas composition for the temperature range of T = 900−1500 K at P = 1 bar are shown in Figure 5, and the results for P = 25 bar are shown in Figure 6. At P = 1 bar, full conversion of methane is achieved at temperatures up to T = 1100 K. By increasing the temperature further, the equilibrium favors conversion of hydrogen and carbon dioxide to water and carbon monoxide. This is in agreement with the equilibrium of the WGS reaction at high temperatures.[36,140,142] In addition, thermodynamic equilibrium favors complete FA decomposition (R4) in this temperature range. This leads to an increase in the mole fractions of water, carbon dioxide, and carbon monoxide compared to the SRM-WGS process. Because the mole fraction of hydrogen is decreasing with the increase in temperature, contrary to the mole fraction of carbon monoxide, different H_2:CO molar ratios are obtained at different temperatures.

Carrying out the SRM-FA process at P = 25 bar changes the equilibrium composition of the reacting system, such that higher temperatures are required to fully reform methane and to reduce the carbon dioxide content in the syngas. This is in agreement with the Le Chatelier's principle[143,144] which states that an increase in the pressure leads to a change in equilibrium composition to a new state in which fewer molecules per mole are present. Here, the thermodynamic equilibrium is shifted toward water, carbon dioxide, and methane (R5) at low temperatures. Therefore, higher temperatures are required to reduce the methane and carbon dioxide concentrations in the syngas.

On the basis of the results shown in Figures 5 and 6, it is clear that the concentrations of hydrogen and carbon monoxide can be adjusted by changing the FA concentration in the reactant feed. To have a clear overview of this principle in Figure 7, the H_2:CO molar ratios in the syngas are plotted as a function of the composition of the reactant feed in the temperature range of T = 800−1500 K at P = 1 and 25 bar. The composition of the reactant feed was obtained by adjusting the HCOOH:H_2O molar ratios between 0.11 and 5.66. Results shown in Figures 7a and 7b correspond to H_2O:CH_4 = 1:1 molar ratio in the reactant feed at P = 1 and 25 bar, respectively. The results shown in Figures 7c and 7d correspond to H_2O:CH_4 = 2:1 molar ratio in the reactant feed at P = 1 and 25 bar, respectively.

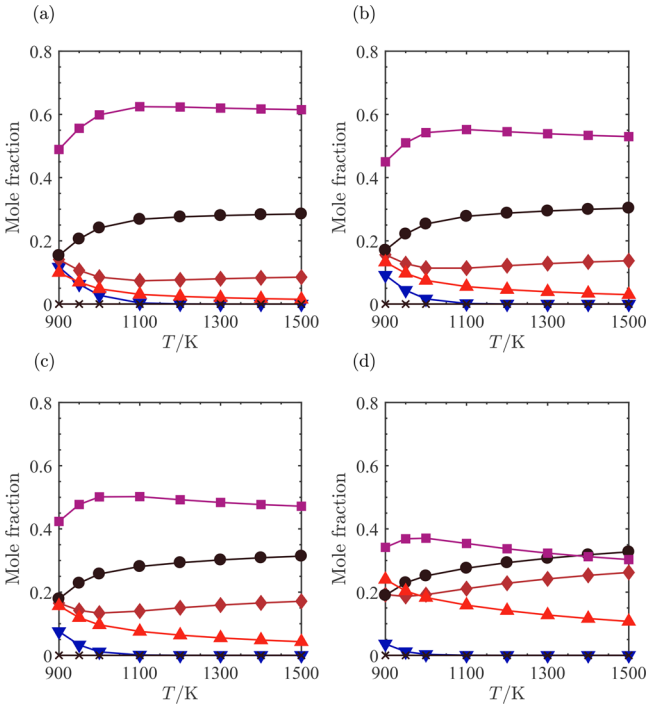

Figure 5. Equilibrium composition of syngas as a function of temperature obtained by cofeeding FA to the SRM reaction at 1 bar and H_2O:CH_4 = 1. The Gibbs minimization method is used to obtain the syngas equilibrium composition using eqs R4 and R5. Initial mole fraction of FA relative to the mole fraction of water: (a) HCOOH:H_2O = 0.49, (b) HCOOH:H_2O = 1.00, (c) HCOOH:H_2O = 1.50, and (d) HCOOH:H_2O = 5.66. In all panels: mole fractions of hydrogen (squares), mole fractions of carbon monoxide (circles), mole fractions of methane (downward-pointing triangles), mole fractions of water (diamonds), mole fractions of carbon dioxide (upward-pointing triangles), and mole fractions of FA (crosses).

Thermochemical equilibrium calculations clearly show that reactions R4 and R5 can be combined to produce syngas with an adjustable H_2:CO molar ratio ranging from one to three. The H_2:CO molar ratio can be adjusted by changing the HCOOH:H_2O:CH_4 ratio in the reactant feed at different temperatures. At high pressures, higher temperatures are required to reduce the concentration of methane and carbon dioxide in the product syngas, as shown in Figure 6. However, adjusting the H_2:CO molar ratio in the syngas can be achieved at any temperature and pressure.

The results show that by feeding FA to the SRM process, the equilibrium composition of the product syngas can be adjusted by changing the concentration of FA in the reactant feed. Future studies should investigate the effect of different types of catalyst for the combined SRM-FA process at different temperatures. The proposed method for adjusting the H_2:CO ratio by using FA is not limited to the methane steam reforming process. First, it can be used in any process where adjustment of the H_2:CO ratio is required (see Figure 1). Examples of this include autothermal reforming, partial oxidation, gas-to-liquid technologies, naphtha reforming, biomass gasification, etc. Second, formic acid can be used for

DOI: 10.1021/acs.iecr.8b02443
Ind. Eng. Chem. Res. 2018, 57, 10663−10674

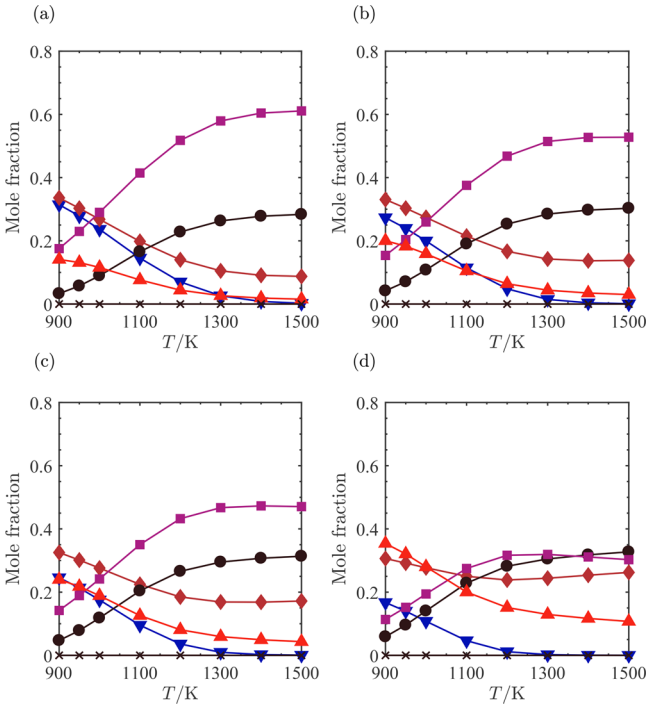

Figure 6. Equilibrium composition of syngas as a function of temperature obtained by cofeeding FA to the SRM reaction at 25 bar and $H_2O:CH_4$ = 1. The Gibbs minimization method is used to obtain the syngas equilibrium composition based on reactions R4 and R5. Initial mole fraction of FA relative to reactions mole fraction of water: (a) $HCOOH:H_2O$ = 0.49, (b) $HCOOH:H_2O$ = 1.00, (c) $HCOOH:H_2O$ = 1.50, and (d) $HCOOH:H_2O$ = 5.66. In all panels: mole fractions of hydrogen (squares), mole fractions of carbon monoxide (circles), mole fractions of methane (downward-pointing triangles), mole fractions of water (diamonds), mole fractions of carbon dioxide (upward-pointing triangles), and mole fractions of FA (crosses).

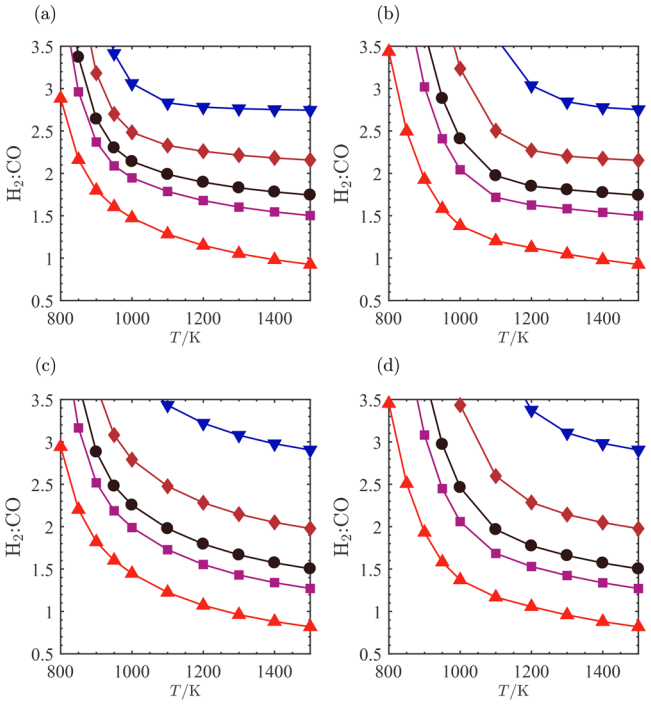

Figure 7. Different equilibrium syngas compositions (H_2:CO ratios) are obtained by cofeeding FA to the SRM reaction at different pressures and temperatures. (a) P = 1 bar, $H_2O:CH_4$ = 1; (b) P = 25 bar, $H_2O:CH_4$ = 1; (c) P = 1 bar, $H_2O:CH_4$ = 2; and (d) P = 25 bar, $H_2O:CH_4$ = 2. In all panels, the initial mole fraction of FA relative to the mole fraction of water: $HCOOH:H_2O$ = 0.11 (downward-pointing triangles), $HCOOH:H_2O$ = 0.49 (diamonds), $HCOOH:H_2O$ = 1.00 (circles), $HCOOH:H_2O$ = 1.50 (squares), and $HCOOH:H_2O$ = 5.66 (upward-pointing triangles).

energy storage by the use of fuel cells and formic acid reformers to generate hydrogen, heat, and electricity.

5. CONCLUSIONS

To adjust the H_2:CO molar ratio during syngas production, FA decomposition can be combined with the steam reforming of methane. The option to use FA as a syngas source is exploited by combining the two FA decomposition reactions at high temperatures. Essentially, FA can be considered as a combined hydrogen and carbon monoxide carrier. Thermodynamic equilibrium calculations show that the syngas composition can be controlled by adjusting the $HCOOH:H_2O:CH_4$ ratio in the reactant feed. It is possible to obtain different H_2:CO molar ratios between 1 and 3 in the product syngas. At higher pressures, higher temperatures are required for complete methane conversion and reducing carbon dioxide content in the syngas. On the basis of our results, it can be concluded that cofeeding FA to the SRM reaction can potentially reduce the traditional SRM and WGS processes from a two-step process to a single-step process able to produce syngas with adjustable H_2:CO ratio. The proposed SMR-FA process based on CO_2 reuse may open up a range of new applications for formic acid.

■ ASSOCIATED CONTENT

Supporting Information

The Supporting Information is available free of charge on the ACS Publications website at DOI: 10.1021/acs.iecr.8b02443.

Computation of the Gibbs free energies of all components (section S1); computation of the Gibbs free energy changes and reaction enthalpies (section S2); Peng–Robinson equation of state (section S3); computed Gibbs free energies of carbon monoxide, water, carbon dioxide, hydrogen, formic acid, and methane (Table S1); critical temperatures, critical pressures, and acentric factors used in the Peng–Robinson equation of state modeling (Table S2) (PDF)

■ AUTHOR INFORMATION

Corresponding Author

*E-mail: t.j.h.vlugt@tudelft.nl (T.J.H.V.).

ORCID

Ahmadreza Rahbari: 0000-0002-6474-3028
Mahinder Ramdin: 0000-0002-8476-7035
Thijs J. H. Vlugt: 0000-0003-3059-8712

Notes

The authors declare no competing financial interest.

DOI: 10.1021/acs.iecr.8b02443
Ind. Eng. Chem. Res. 2018, 57, 10663−10674

■ ACKNOWLEDGMENTS

This work was sponsored by NWO Exacte Wetenschappen (Physical Sciences) for the use of supercomputer facilities, with financial support from the Nederlandse Organisatie voor Wetenschappelijk Onderzoek (Netherlands Organization for Scientific Research, NWO). T.J.H.V. acknowledges NWO-CW for a VICI grant.

■ REFERENCES

(1) Buttler, A.; Spliethoff, H. Current status of water electrolysis for energy storage, grid balancing and sector coupling via power-to-gas and power-to-liquids: A review. *Renewable Sustainable Energy Rev.* **2018**, *82*, 2440−2454.

(2) Riese, J.; Grünewald, M.; Lier, S. Utilization of renewably generated power in the chemical process industry. *Energy Sust. Soc.* **2014**, *4*, 18.

(3) Schiffer, Z. J.; Manthiram, K. Electrification and decarbonization of the chemical industry. *Joule* **2017**, *1*, 10−14.

(4) Alvarez, A.; Bansode, A.; Urakawa, A.; Bavykina, A. V.; Wezendonk, T. A.; Makkee, M.; Gascon, J.; Kapteijn, F. Challenges in the greener production of formates/formic acid, methanol, and DME by heterogeneously catalyzed CO_2 hydrogenation Processes. *Chem. Rev.* **2017**, *117*, 9804−9838.

(5) Goeppert, A.; Czaun, M.; Jones, J.-P.; Surya Prakash, G. K.; Olah, G. A. Recycling of carbon dioxide to methanol and derived products - closing the loop. *Chem. Soc. Rev.* **2014**, *43*, 7995−8048.

(6) Centi, G.; Perathoner, S. Opportunities and prospects in the chemical recycling of carbon dioxide to fuels. *Catal. Today* **2009**, *148*, 191−205.

(7) Centi, G.; Quadrelli, E. A.; Perathoner, S. Catalysis for CO_2 conversion: a key technology for rapid introduction of renewable energy in the value chain of chemical industries. *Energy Environ. Sci.* **2013**, *6*, 1711−1731.

(8) Leitner, W. Carbon dioxide as a raw Material: the synthesis of formic acid and its derivatives from CO_2. *Angew. Chem., Int. Ed. Engl.* **1995**, *34*, 2207−2221.

(9) Kortlever, R.; Peters, I.; Koper, S.; Koper, M. T. M. Electrochemical CO_2 reduction to formic acid at low overpotential and with high faradaic efficiency on carbon-supported bimetallic Pd-Pt nanoparticles. *ACS Catal.* **2015**, *5*, 3916−3923.

(10) Natsui, K.; Iwakawa, H.; Ikemiya, N.; Nakata, K.; Einaga, Y. Stable and highly efficient electrochemical production of formic acid from carbon dioxide using diamond electrodes. *Angew. Chem., Int. Ed.* **2018**, *57*, 2639−2643.

(11) Lee, S.; Ju, H.; Machunda, R.; Uhm, S.; Lee, J. K.; Lee, H. J.; Lee, J. Sustainable production of formic acid by electrolytic reduction of gaseous carbon dioxide. *J. Mater. Chem. A* **2015**, *3*, 3029−3034.

(12) Chaplin, R.; Wragg, A. Effects of process conditions and electrode material on reaction pathways for carbon dioxide electroreduction with particular reference to formate formation. *J. Appl. Electrochem.* **2003**, *33*, 1107−1123.

(13) Lu, X.; Leung, D. Y. C.; Wang, H.; Leung, M. K. H.; Xuan, J. Electrochemical decrease in carbon dioxide to formic acid. *ChemElectroChem* **2014**, *1*, 836−849.

(14) Chen, A.; Lin, B.-L. A simple framework for quantifying electrochemical CO_2 fixation. *Joule* **2018**, *2*, 594−606.

(15) Thorson, M. R.; Siil, K. I.; Kenis, P. J. Effect of cations on the electrochemical conversion of CO_2 to CO. *J. Electrochem. Soc.* **2013**, *160*, F69−F74.

(16) Jouny, M.; Luc, W.; Jiao, F. General techno-economic analysis of CO_2 electrolysis systems. *Ind. Eng. Chem. Res.* **2018**, *57*, 2165−2177.

(17) Steinberg, M. Modern and prospective technologies for hydrogen production from fossil fuels. *Int. J. Hydrogen Energy* **1989**, *14*, 797−820.

(18) Moret, S.; Dyson, P. J.; Laurenczy, G. Direct synthesis of formic acid from carbon dioxide by hydrogenation in acidic media. *Nat. Commun.* **2014**, *5*, 4017.

(19) Tedsree, K.; Li, T.; Jones, S.; Chan, C. W. A.; Yu, K. M. K.; Bagot, P. A.; Marquis, E. A.; Smith, G. D.; Tsang, S. C. E. Hydrogen production from formic acid decomposition at room temperature using a Ag-Pd core-shell nanocatalyst. *Nat. Nanotechnol.* **2011**, *6*, 302.

(20) Yoshida, K.; Wakai, C.; Matubayasi, N.; Nakahara, M. NMR spectroscopic evidence for an intermediate of formic acid in the water-gas-shift Reaction. *J. Phys. Chem. A* **2004**, *108*, 7479−7482.

(21) Xing, R.; Qi, W.; Huber, G. W. Production of furfural and carboxylic acids from waste aqueous hemicellulose solutions from the pulp and paper and cellulosic ethanol industries. *Energy Environ. Sci.* **2011**, *4*, 2193−2205.

(22) Jin, F.; Enomoto, H. Rapid and highly selective conversion of biomass into value-added products in hydrothermal conditions: chemistry of acid/base-catalysed and oxidation reactions. *Energy Environ. Sci.* **2011**, *4*, 382−397.

(23) Kamm, B.; Gruber, P. R.; Kamm, M. *Biorefineries-Industrial Processes and Products*; Wiley Online Library: WILEY-VCH Verlag GmbH & Co. KGaA: Weinheim, Germany, 2007.

(24) Schaub, T.; Paciello, R. A. A process for the synthesis of formic acid by CO_2 hydrogenation: thermodynamic aspects and the role of CO. *Angew. Chem., Int. Ed.* **2011**, *50*, 7278−7282.

(25) Bulushev, D. A.; Ross, J. R. H. Towards sustainable production of formic acid. *ChemSusChem* **2018**, *11*, 821−836.

(26) Bernskoetter, W. H.; Hazari, N. Reversible hydrogenation of carbon dioxide to formic acid and methanol: Lewis acid enhancement of base metal catalysts. *Acc. Chem. Res.* **2017**, *50*, 1049−1058.

(27) Saito, K.; Shiose, T.; Takahashi, O.; Hidaka, Y.; Aiba, F.; Tabayashi, K. Unimolecular decomposition of formic acid in the gas phase on the ratio of the competing reaction channels. *J. Phys. Chem. A* **2005**, *109*, 5352−5357.

(28) Saito, K.; Kakumoto, T.; Kuroda, H.; Torii, S.; Imamura, A. Thermal unimolecular decomposition of formic acid. *J. Chem. Phys.* **1984**, *80*, 4989−4996.

(29) Columbia, M.; Thiel, P. The interaction of formic acid with transition metal surfaces, studied in ultrahigh vacuum. *J. Electroanal. Chem.* **1994**, *369*, 1−14.

(30) Iglesia, E.; Boudart, M. Decomposition of formic acid on copper, nickel, and copper-nickel alloys: III. Catalytic decomposition on nickel and copper-nickel alloys. *J. Catal.* **1983**, *81*, 224−238.

(31) Iglesia, E.; Boudart, M. Decomposition of formic acid on copper, nickel, and copper-nickel alloys: I. Preparation and characterization of catalysts. *J. Catal.* **1983**, *81*, 204−213.

(32) Iglesia, E.; Boudart, M. Decomposition of formic acid on copper, nickel, and copper-nickel alloys: II. Catalytic and temperature-programmed decomposition of formic acid on $CuSiO_2$, $CuAl_2O_3$, and Cu powder. *J. Catal.* **1983**, *81*, 214−223.

(33) Iglesia, E. Unimolecular and bimolecular formic acid decomposition on copper. *J. Phys. Chem.* **1986**, *90*, 5272−5274.

(34) Herron, J. A.; Scaranto, J.; Ferrin, P.; Li, S.; Mavrikakis, M. Trends in formic acid decomposition on model transition metal surfaces: a density functional theory study. *ACS Catal.* **2014**, *4*, 4434−4445.

(35) Lee, H. J.; Kang, D.-C.; Pyen, S. H.; Shin, M.; Suh, Y.-W.; Han, H.; Shin, C.-H. Production of H_2-free CO by decomposition of formic acid over ZrO_2 catalysts. *Appl. Catal., A* **2017**, *531*, 13−20.

(36) Yu, J.; Savage, P. E. Decomposition of formic acid under hydrothermal conditions. *Ind. Eng. Chem. Res.* **1998**, *37*, 2−10.

(37) Bjerre, A. B.; Soerensen, E. Thermal decomposition of dilute aqueous formic acid solutions. *Ind. Eng. Chem. Res.* **1992**, *31*, 1574−1577.

(38) Müller, K.; Brooks, K.; Autrey, T. Hydrogen storage in formic acid: a comparison of process options. *Energy Fuels* **2017**, *31*, 12603−12611.

(39) López, F.; Stone, F. Formic acid decomposition over α-Chromia-Alumina solid solution catalysts. *Z. Phys. Chem.* **1978**, *111*, 247−256.

(40) Wescott, B. B.; Engelder, C. J. The catalytic decomposition of formic acid. *J. Phys. Chem.* **1925**, *30*, 476−479.

DOI: 10.1021/acs.iecr.8b02443
Ind. Eng. Chem. Res. 2018, 57, 10663−10674

(41) Blake, P.; Hinshelwood Cyril norman, P. The homogeneous decomposition reactions of gaseous formic acid. *Proc. R. Soc. London A: Math., Phys. Eng. Sci.* **1960**, *255*, 444−455.
(42) Blake, P. G.; Davies, H. H.; Jackson, G. E. Dehydration mechanisms in the thermal decomposition of gaseous formic acid. *J. Chem. Soc. B* **1971**, 1923−1925.
(43) Hinshelwood, C. N.; Topley, B. CXV.-The energy of activation in heterogeneous gas reactions with relation to the thermal decomposition of formic acid vapour. *J. Chem. Soc., Trans.* **1923**, *123*, 1014−1025.
(44) Hinshelwood, C. N.; Hartley, H.; Topley, B. The influence of temperature on two alternative modes of decomposition of formic acid. *Proc. R. Soc. London, Ser. A* **1922**, *100*, 575−581.
(45) Wakai, C.; Yoshida, K.; Tsujino, Y.; Matubayasi, N.; Nakahara, M. Effect of concentration, acid, temperature, and metal on competitive reaction pathways for decarbonylation and decarboxylation of formic acid in hot water. *Chem. Lett.* **2004**, *33*, 572−573.
(46) Bröll, D.; Kaul, C.; Krämer, A.; Krammer, P.; Richter, T.; Jung, M.; Vogel, H.; Zehner, P. Chemistry in supercritical water. *Angew. Chem., Int. Ed.* **1999**, *38*, 2998−3014.
(47) Grasemann, M.; Laurenczy, G. Formic acid as a hydrogen source - recent developments and future trends. *Energy Environ. Sci.* **2012**, *5*, 8171−8181.
(48) Zhu, Q.-L.; Tsumori, N.; Xu, Q. Immobilizing extremely catalytically active palladium nanoparticles to carbon nanospheres: a weakly-capping growth approach. *J. Am. Chem. Soc.* **2015**, *137*, 11743−11748.
(49) Henricks, V.; Yuranov, I.; Autissier, N.; Laurenczy, G. Dehydrogenation of formic acid over a homogeneous Ru-TPPTS catalyst: unwanted CO production and its successful removal by PROX. *Catalysts* **2017**, *7*, 348.
(50) Newsome, D. S. The water-gas shift reaction. *Catal. Rev.: Sci. Eng.* **1980**, *21*, 275−318.
(51) Moulijn, J. A.; Makkee, M.; Van Diepen, A. E. *Chemical Process Technology*, 2nd ed.; John Wiley & Sons: West Sussex, UK, 2013.
(52) Rostrup-Nielsen, J. R.; Sehested, J.; Norskov, J. K. Hydrogen and synthesis gas by steam- and CO_2 reforming. *Adv. Catal.* **2002**, *47*, 65−139.
(53) Roh, H. S.; Koo, K. Y.; Jeong, J. H.; Seo, Y. T.; Seo, D. J.; Seo, Y. S.; Yoon, W. L.; Park, S. B. Combined reforming of methane over supported Ni catalysts. *Catal. Lett.* **2007**, *117*, 85−90.
(54) Rostrup-Nielsen, J. R. *Catalysis: Science and Technology*; Springer: Berlin, 1984; Vol. *5*, pp 1−117.
(55) Roh, H. S.; Jun, K. W.; Dong, W. S.; Chang, J. S.; Park, S. E.; Joe, Y. I. Highly active and stable Ni/Ce-ZrO_2 catalyst for H_2 production from methane. *J. Mol. Catal. A: Chem.* **2002**, *181*, 137−142.
(56) Pena, M.; Gomez, J.; Fierro, J. New catalytic routes for syngas and hydrogen production. *Appl. Catal., A* **1996**, *144*, 7−57.
(57) Song, X.; Guo, Z. Technologies for direct production of flexible H_2/CO synthesis gas. *Energy Convers. Manage.* **2006**, *47*, 560−569.
(58) LeValley, T. L.; Richard, A. R.; Fan, M. The progress in water gas shift and steam reforming hydrogen production technologies - a review. *Int. J. Hydrogen Energy* **2014**, *39*, 16983−17000.
(59) Sehested, J. Four challenges for nickel steam-reforming catalysts. *Catal. Today* **2006**, *111*, 103−110.
(60) Schwab, G.-M.; Schwab-Agallidis, E. On selective catalysis. *J. Am. Chem. Soc.* **1949**, *71*, 1806−1816.
(61) Hietala, J.; Vuori, A.; Johnsson, P.; Pollari, I.; Reutemann, W.; Kieczka, H. *Ullmann's Encyclopedia of Industrial Chemistry*; American Cancer Society: 2016; pp 1−22.
(62) Zhao, Z.; Chen, Z.; Lu, G. Computational discovery of Nickel-based catalysts for CO_2 reduction to formic acid. *J. Phys. Chem. C* **2017**, *121*, 20865−20870.
(63) Yoo, J. S.; Abild-Pedersen, F.; Norskov, J. K.; Studt, F. Theoretical analysis of transition-metal catalysts for formic acid decomposition. *ACS Catal.* **2014**, *4*, 1226−1233.
(64) Trillo, J. M.; Munuera, G.; Criado, J. M. Catalytic decomposition of formic acid on metal oxides. *Catal. Rev.: Sci. Eng.* **1972**, *7*, 51−86.
(65) Boddien, A.; Gärtner, F.; Federsel, C.; Sponholz, P.; Mellmann, D.; Jackstell, R.; Junge, H.; Beller, M. CO_2-"neutral" hydrogen storage based on bicarbonates and formates. *Angew. Chem., Int. Ed.* **2011**, *50*, 6411−6414.
(66) Yu, X.; Pickup, P. G. Recent advances in direct formic acid fuel cells (DFAFC). *J. Power Sources* **2008**, *182*, 124−132.
(67) Liu, Z.; Hong, L.; Tham, M. P.; Lim, T. H.; Jiang, H. Nanostructured Pt/C and Pd/C catalysts for direct formic acid fuel cells. *J. Power Sources* **2006**, *161*, 831−835.
(68) Kundu, A.; Jang, J.; Gil, J.; Jung, C.; Lee, H.; Kim, S.-H.; Ku, B.; Oh, Y. Micro-fuel cells-current development and applications. *J. Power Sources* **2007**, *170*, 67−78.
(69) Piola, L.; Fernandez-Salas, J. A.; Nahra, F.; Poater, A.; Cavallo, L.; Nolan, S. P. Ruthenium-catalysed decomposition of formic acid: fuel cell and catalytic applications. *Mol. Catal.* **2017**, *440*, 184−189.
(70) Schnabel, T.; Cortada, M.; Vrabec, J.; Lago, S.; Hasse, H. Molecular model for formic acid adjusted to vapor-liquid equilibria. *Chem. Phys. Lett.* **2007**, *435*, 268−272.
(71) Mura, M. G.; Luca, L. D.; Giacomelli, G.; Porcheddu, A. Formic acid: a promising bio-renewable feedstock for fine chemicals. *Adv. Synth. Catal.* **2012**, *354*, 3180−3186.
(72) Chang, T.; Rousseau, R. W.; Kilpatrick, P. K. Methanol synthesis reactions: calculations of equilibrium conversions using equations of state. *Ind. Eng. Chem. Process Des. Dev.* **1986**, *25*, 477−481.
(73) Hindermann, J. P.; Hutchings, G. J.; Kiennemann, A. Mechanistic aspects of the formation of hydrocarbons and alcohols from CO hydrogenation. *Catal. Rev.: Sci. Eng.* **1993**, *35*, 1−127.
(74) Dry, M. E. The Fischer−Tropsch process: 1950−2000. *Catal. Today* **2002**, *71*, 227−241.
(75) Schulz, H. Short history and present trends of Fischer−Tropsch synthesis. *Appl. Catal., A* **1999**, *186*, 3−12.
(76) Roh, H. S.; Koo, K. Y.; Joshi, U. D.; Yoon, W. L. Combined H_2O and CO_2 reforming of methane over Ni-Ce-ZrO_2 catalysts for gas to liquids (GTL). *Catal. Lett.* **2008**, *125*, 283−288.
(77) Jang, W. J.; Jeong, D. W.; Shim, J. O.; Roh, H. S.; Son, I. H.; Lee, S. J. H_2 and CO production over a stable Ni-MgO-$Ce_{0.8}Zr_{0.2}O_2$ catalyst from CO_2 reforming of CH_4. *Int. J. Hydrogen Energy* **2013**, *38*, 4508−4512.
(78) Roh, H. S.; Jun, K. W. Carbon dioxide reforming of methane over Ni catalysts supported on Al_2O_3 modified with, La_2O_3, MgO, and CaO. *Catal. Surv. Asia* **2008**, *12*, 239−252.
(79) Choudhary, V. R.; Mammon, A. S.; Sansare, S. D. Selective oxidation of methane to CO and H_2 over Ni/MgO at low temperatures. *Angew. Chem., Int. Ed. Engl.* **1992**, *31*, 1189−1190.
(80) Dong, W.-S.; Roh, H.-S.; Jun, K.-W.; Park, S.-E.; Oh, Y.-S. Methane reforming over Ni/Ce-ZrO_2 catalysts: effect of nickel content. *Appl. Catal., A* **2002**, *226*, 63−72.
(81) Roh, H.-S.; Jun, K.-W.; Dong, W.-S.; Park, S.-E.; Joe, Y.-I. Partial oxidation of methane over Ni/θ-Al_2O_3 Catalysts. *Chem. Lett.* **2001**, *30*, 666−667.
(82) Knifton, J. F. Syngas reactions: IX. Acetic acid from synthesis gas. *J. Catal.* **1985**, *96*, 439−453.
(83) Choudhary, V. R.; Mondal, K. C. CO_2 reforming of methane combined with steam reforming or partial oxidation of methane to syngas over $NdCoO_3$ perovskite-type mixed metal-oxide catalyst. *Appl. Energy* **2006**, *83*, 1024−1032.
(84) Cai, X.; Cai, Y.; Lin, W. Autothermal reforming of methane over Ni catalysts supported over ZrO_2-CeO_2-Al_2O_3. *J. Nat. Gas Chem.* **2008**, *17*, 201−207.
(85) Cai, X.; Dong, X.; Lin, W. Autothermal reforming of methane over Ni catalysts supported on CuO-ZrO_2-CeO_2-Al_2O_3. *J. Nat. Gas Chem.* **2006**, *15*, 122−126.
(86) Olah, G. A.; Goeppert, A.; Prakash, G. K. S. Chemical recycling of carbon dioxide to methanol and dimethyl ether: from greenhouse

DOI: 10.1021/acs.iecr.8b02443
Ind. Eng. Chem. Res. 2018, 57, 10663−10674

gas to renewable, environmentally carbon neutral fuels and synthetic hydrocarbons. *J. Org. Chem.* **2009**, *74*, 487−498.
(87) Byrne, P., Jr.; Gohr, E.; Haslam, R. Recent progress in hydrogenation of petroleum. *Ind. Eng. Chem.* **1932**, *24*, 1129−1135.
(88) Tsang, S.; Claridge, J.; Green, M. Recent advances in the conversion of methane to synthesis gas. *Catal. Today* **1995**, *23*, 3−15.
(89) Vermeiren, W.; Blomsma, E.; Jacobs, P. Catalytic and thermodynamic approach of the oxyreforming reaction of methane. *Catal. Today* **1992**, *13*, 427−436.
(90) Van Beurden, P. *On the Catalytic Aspects of Steam-Methane Reforming*; Energy Research Centre of the Netherlands (ECN): Technical Report I-04-003, 2004.
(91) Jeong, J. H.; Lee, J. W.; Seo, D. J.; Seo, Y.; Yoon, W. L.; Lee, D. K.; Kim, D. H. Ru-doped Ni catalysts effective for the steam reforming of methane without the pre-reduction treatment with H_2. *Appl. Catal., A* **2006**, *302*, 151−156.
(92) Wang, S.; Lu, G. Q. M.; Millar, G. J. Carbon dioxide reforming of methane To produce synthesis gas over metal-supported catalysts: state of the art. *Energy Fuels* **1996**, *10*, 896−904.
(93) Koo, K. Y.; Roh, H.-S.; Seo, Y. T.; Seo, D. J.; Yoon, W. L.; Park, S. B. A highly effective and stable nano-sized Ni/MgO-Al_2O_3 catalyst for gas to liquids (GTL) process. *Int. J. Hydrogen Energy* **2008**, *33*, 2036−2043.
(94) Qin, D.; Lapszewicz, J.; Jiang, X. Comparison of partial oxidation and steam-CO_2 mixed reformingof CH_4 to syngas on MgO-supported metals. *J. Catal.* **1996**, *159*, 140−149.
(95) Graaf, G. H.; Winkelman, J. G. Chemical equilibria in methanol synthesis including the water-gas shift reaction: a critical reassessment. *Ind. Eng. Chem. Res.* **2016**, *55*, 5854−5864.
(96) Graaf, G.; Sijtsema, P.; Stamhuis, E.; Joosten, G. Chemical equilibria in methanol synthesis. *Chem. Eng. Sci.* **1986**, *41*, 2883−2890.
(97) Wang, S.; Lu, G. Q. M. Catalytic activities and coking characteristics of oxides-supported Ni catalysts for CH_4 reforming with carbon dioxide. *Energy Fuels* **1998**, *12*, 248−256.
(98) Oh, Y. S.; Roh, H. S.; Jun, K. W.; Baek, Y. S. A highly active catalyst, Ni/Ce-ZrO_2/θ-Al_2O_3, for on-site H_2 generation by steam methane reforming: pretreatment effect. *Int. J. Hydrogen Energy* **2003**, *28*, 1387−1392.
(99) Hou, Z.; Chen, P.; Fang, H.; Zheng, X.; Yashima, T. Production of synthesis gas via methane reforming with CO_2 on noble metals and small amount of noble-(Rh-) promoted Ni catalysts. *Int. J. Hydrogen Energy* **2006**, *31*, 555−561.
(100) Rostrupnielsen, J.; Hansen, J. CO_2-reforming of methane over transition metals. *J. Catal.* **1993**, *144*, 38−49.
(101) Ross, J.; van Keulen, A.; Hegarty, M.; Seshan, K. The catalytic conversion of natural gas to useful products. *Catal. Today* **1996**, *30*, 193−199.
(102) Bradford, M. C. J.; Vannice, M. A. CO_2 reforming of CH_4. *Catal. Rev.: Sci. Eng.* **1999**, *41*, 1−42.
(103) Ashcroft, A.; Cheetham, A.; Green, M.; Vernon, P. D. F. Partial oxidation of methane to synthesis gas using carbon dioxide. *Nature* **1991**, *352*, 225−226.
(104) Claridge, J. B.; Green, M. L. H.; Tsang, S. C.; York, A. P. E.; Ashcroft, A. T.; Battle, P. D. A study of carbon deposition on catalysts during the partial oxidation of methane to synthesis gas. *Catal. Lett.* **1993**, *22*, 299−305.
(105) Jiang, H.; Li, H.; Zhang, Y. Tri-reforming of methane to syngas over Ni/Al_2O_3-Thermal distribution in the catalyst bed. *J. Fuel Chem. Technol.* **2007**, *35*, 72−78.
(106) Dissanayake, D.; Rosynek, M. P.; Kharas, K. C.; Lunsford, J. H. Partial oxidation of methane to carbon monoxide and hydrogen over a Ni/Al_2O_3 catalyst. *J. Catal.* **1991**, *132*, 117−127.
(107) Ashcroft, A.; Cheetham, A.; Foord, J. A.; Green, M.; Grey, C.; Murrell, A.; Vernon, P. D. F. Selective oxidation of methane to synthesis gas using transition metal catalysts. *Nature* **1990**, *344*, 319−321.
(108) Koo, K. Y.; Roh, H.-S.; Jung, U. H.; Yoon, W. L. CeO_2 Promoted Ni/Al_2O_3 catalyst in combined steam and carbon dioxide reforming of methane for gas to liquid (GTL) process. *Catal. Lett.* **2009**, *130*, 217−221.
(109) Jing, Q.; Lou, H.; Fei, J.; Hou, Z.; Zheng, X. Syngas production from reforming of methane with CO_2 and O_2 over Ni/SrO-SiO_2 catalysts in a fluidized bed reactor. *Int. J. Hydrogen Energy* **2004**, *29*, 1245−1251.
(110) Prettre, M.; Eichner, C.; Perrin, M. The catalytic oxidation of methane to carbon monoxide and hydrogen. *Trans. Faraday Soc.* **1946**, *42*, 335b−339.
(111) Yoshitomi, S.; Morita, Y.; Yamamoto, K. Catalytic partial oxidation of hydrocarbons at high temperature. *Bull. Jpn. Pet. Inst.* **1962**, *4*, 15−27.
(112) Song, C.; Pan, W. Tri-reforming of methane: a novel concept for catalytic production of industrially useful synthesis gas with desired H_2/CO ratios. *Catal. Today* **2004**, *98*, 463−484.
(113) Yoo, J.; Bang, Y.; Han, S. J.; Park, S.; Song, J. H.; Song, I. K. Hydrogen production by tri-reforming of methane over nickel-alumina aerogel catalyst. *J. Mol. Catal. A: Chem.* **2015**, *410*, 74−80.
(114) Halmann, M.; Steinfeld, A. Thermoneutral tri-reforming of flue gases from coal- and gas-fired power stations. *Catal. Today* **2006**, *115*, 170−178.
(115) Lee, S. H.; Cho, W.; Ju, W.-S.; Cho, B. H.; Lee, Y. C.; Baek, Y. S. Tri-reforming of CH_4 using CO_2 for production of synthesis gas to dimethyl ether. *Catal. Today* **2003**, *87*, 133−137.
(116) Choudhary, V. R.; Rajput, A. M. Simultaneous carbon dioxide and steam reforming of methane to syngas over NiO-CaO catalyst. *Ind. Eng. Chem. Res.* **1996**, *35*, 3934−3939.
(117) Zhang, Q.-H.; Li, Y.; Xu, B.-Q. Reforming of methane and coalbed methane over nanocomposite Ni/ZrO_2 catalyst. *Catal. Today* **2004**, *98*, 601−605.
(118) Pompeo, F.; Nichio, N. N.; Ferretti, O. A.; Resasco, D. Study of Ni catalysts on different supports to obtain synthesis gas. *Int. J. Hydrogen Energy* **2005**, *30*, 1399−1405.
(119) Walas, S. M. *Phase Equilibria in Chemical Engineering*; Butterworth-Heinemann: USA, 1985.
(120) Krieger, F. J.; White, W. B. A Simplified method for computing the equilibrium composition of gaseous systems. *J. Chem. Phys.* **1948**, *16*, 358−360.
(121) Brinkley, S. R., Jr. Calculation of the equilibrium composition of systems of many constituents. *J. Chem. Phys.* **1947**, *15*, 107−110.
(122) Smith, J. M.; Van Ness, H. C.; Abbott, M. M. *Introduction to Chemical Engineering Thermodynamics*, 7th ed.; McGraw-Hill: New York, 2005.
(123) Smith, W. R. The computation of chemical equilibria in complex systems. *Ind. Eng. Chem. Fundam.* **1980**, *19*, 1−10.
(124) Gmehling, J.; Kolbe, B.; Kleiber, M.; Rarey, J. *Chemical Thermodynamics for Process Simulation*, 1st ed.; Wiley-VCH Verlag & GmbH Co. KGaA: Weinheim, Germany, 2012.
(125) Stone, E. Complex chemical equilibria: application of Newton-Raphson method to solve non-linear equations. *J. Chem. Educ.* **1966**, *43*, 241−244.
(126) McQuarrie, D. A.; Simon, J. D. *Physical Chemistry: A Molecular Approach*, 1st ed.; University Science Books: Sausalito, CA, 1997.
(127) Hill, T. L. *An Introduction to Statistical Thermodynamics*, 1st ed.; Dover Publications Inc.: New York, 2015.
(128) Balaji, S. P.; Gangarapu, S.; Ramdin, M.; Torres-Knoop, A.; Zuilhof, H.; Goetheer, E. L.; Dubbeldam, D.; Vlugt, T. J. H. Simulating the reactions of CO_2 in aqueous monoethanolamine solution by reaction ensemble Monte Carlo using the Continuous Fractional Component Method. *J. Chem. Theory Comput.* **2015**, *11*, 2661−2669.
(129) Poursaeidesfahani, A.; Hens, R.; Rahbari, A.; Ramdin, M.; Dubbeldam, D.; Vlugt, T. J. H. Efficient application of Continuous Fractional Component Monte Carlo in the reaction ensemble. *J. Chem. Theory Comput.* **2017**, *13*, 4452−4466.
(130) Sandler, S. I. *Chemical, Biochemical, and Engineering Thermodynamics*, 4th ed.; John Wiley & Sons: New York, 2017.

DOI: 10.1021/acs.iecr.8b02443
Ind. Eng. Chem. Res. 2018, 57, 10663−10674

(131) Moran, M. J.; Shapiro, H. N. *Fundamentals of Engineering Thermodynamics*, 5th ed.; John Wiley & Sons: West Sussex, England, 2006.
(132) Rahbari, A.; Hens, R.; Nikolaidis, I. K.; Poursaeidesfahani, A.; Ramdin, M.; Economou, I. G.; Moultos, O. A.; Dubbeldam, D.; Vlugt, T. J. H. Computation of partial molar properties using Continuous Fractional Component Monte Carlo. *Mol. Phys.*, in press.
(133) Michelsen, M.; Möllerup, J. M. *Thermodynamic Models: Fundamental & Computational Aspects*, 2nd ed.; Tie-Line Publications: Holte, Denmark, 2007.
(134) *Optimization Toolbox UserMPSaposs Guide*; MathWorks, Inc.: Natick, MA, 2016.
(135) Peng, D.-Y.; Robinson, D. B. A new two-constant equation of state. *Ind. Eng. Chem. Fundam.* **1976**, *15*, 59−64.
(136) Kontogeorgis, G. M.; Folas, G. K. *Thermodynamic Models for Industrial Applications: from Classical and Advanced Mixing Rules to Association Theories*, 1st ed.; John Wiley & Sons: Wiltshire, Great Britain, 2009.
(137) Kwak, T.; Mansoori, G. A. Van der Waals mixing rules for cubic equations of state. Applications for supercritical fluid extraction modelling. *Chem. Eng. Sci.* **1986**, *41*, 1303−1309.
(138) Lin, C.-T.; Daubert, T. E. Estimation of partial molar volume and fugacity coefficient of components in mixtures from the soave and Peng-Robinson equations of state. *Ind. Eng. Chem. Process Des. Dev.* **1980**, *19*, 51−59.
(139) Bustamante, F.; Enick, R. M.; Cugini, A.; Killmeyer, R. P.; Howard, B. H.; Rothenberger, K. S.; Ciocco, M. V.; Morreale, B. D.; Chattopadhyay, S.; Shi, S. High-temperature kinetics of the homogeneous reverse water-gas shift reaction. *AIChE J.* **2004**, *50*, 1028−1041.
(140) Joo, O.-S.; Jung, K.-D.; Moon, I.; Rozovskii, A. Y.; Lin, G. I.; Han, S.-H.; Uhm, S.-J. Carbon dioxide hydrogenation to form methanol via a reverse-water-gas-shift reaction (the CAMERE process). *Ind. Eng. Chem. Res.* **1999**, *38*, 1808−1812.
(141) Callaghan, C. A. Kinetics and catalysis of the water-gas-shift reaction: A microkinetic and graph theoretic approach. Ph.D. Thesis, Worcester Polytechnic Institute, Worcester, MA, 2006.
(142) Tingey, G. Kinetics of the water-gas equilibrium Reaction. I. the reaction of carbon dioxide with hydrogen. *J. Phys. Chem.* **1966**, *70*, 1406−1412.
(143) De Heer, J. The principle of Le Châtelier and Braun. *J. Chem. Educ.* **1957**, *34*, 375.
(144) Campbell, J. A. Le Châtelier's principle, temperature effects, and entropy. *J. Chem. Educ.* **1985**, *62*, 231.
(145) Wender, I. Reactions of synthesis gas. *Fuel Process. Technol.* **1996**, *48*, 189−297.
(146) Ajmera, S. K.; Losey, M. W.; Jensen, K. F.; Schmidt, M. A. Microfabricated packed-bed reactor for phosgene synthesis. *AIChE J.* **2001**, *47*, 1639−1647.

DOI: 10.1021/acs.iecr.8b02443
Ind. Eng. Chem. Res. 2018, 57, 10663−10674